Thermodynamics of the Fragile X Mental Retardation Protein RGG Box Interactions with G Quartet Forming RNA†

Kimberly J. Zanotti,‡,§ Patrick E. Lackey,‡,§ Genevieve L. Evans,|| and Mihaela-Rita Mihailescu*,§

Department of Chemistry and Biochemistry, Duquesne University, Pittsburgh, Pennsylvania 15282, and Department of Chemistry, Acadia University, Wolfville, Nova Scotia, Canada

Received February 1, 2006; Revised Manuscript Received May 1, 2006

ABSTRACT: Fragile X syndrome, the most common form of inherited mental retardation, is the result of an unstable expansion of a CGG trinucleotide repeat in the 5′ UTR of the fragile X mental retardation-1 (*FMR1*) gene. The abnormal hypermethylation of the expanded CGG repeats causes the transcriptional silencing of the *FMR1* gene and, consequently, the loss of the fragile X mental retardation protein (FMRP). FMRP is an RNA binding protein that binds to G quartet forming RNA using its RGG box motif. In this study we have performed a thermodynamic analysis of the interactions between the FMRP RGG box domain and Sc1, an RNA molecule which had been previously shown to be bound with high affinity by both the full-length FMRP and by its RGG box domain. We have determined that the association between the FMRP RGG box and Sc1 RNA is dominated by hydrophobic and hydrogen bond interactions, with minor contributions from electrostatic interactions, and that the FMRP RGG box binding increases the stability of the G quartet RNA structure significantly. Interestingly, we found that the G quartet recognition is necessary but not sufficient for the FMRP RGG box binding to this RNA target, indicating that additional interactions of the peptide, possibly with the stem and/or stem−G quartet junction region, are required. Our results also indicate that the G quartet RNA recognition is not a general feature of the RGG box motif but rather carries some sequence, protein and/or RNA, specificity.

Fragile X syndrome is the most common form of inherited mental retardation, affecting ∼1 in 4000 males and ∼1 in 8000 females (*1*). The syndrome is the result of an unstable expansion of a CGG trinucleotide repeat in the 5′ UTR of the fragile X mental retardation-1 *(FMR1)* gene (reviewed in ref *2*). When the CGG expansion repeats exceed ∼230, they are abnormally hypermethylated, causing the transcriptional silencing of the *FMR1* gene and, consequently, the loss of the fragile X mental retardation protein (FMRP). FMRP is produced in many tissues, with its most abundant expression occurring in brain and testes (*3*). In neurons, FMRP is present both in the cell body and at the synapses (reviewed in ref *4*). FMRP is an RNA binding protein that has two types of RNA binding domains: two K homology (KH) domains and an arginine−glycine−glycine-rich domain, the RGG box. In addition, the protein has a nuclear localization signal (NLS) at its N-terminus and a nuclear export signal (NES) at its C-terminus, being able to shuttle between the nucleus and cytoplasm (*5*, *6*). More recently, a new independently folded domain which is believed to be involved in the interactions of FMRP with its protein partners has been isolated in the N-terminal part of FMRP (*7*, *8*). The current model for FMRP function is that it binds to specific messenger RNA (mRNA) targets in the nucleus, being involved in the transport and translation regulation of these mRNAs (*9*). FMRP was found to be associated with actively translating polyribosomes in various nonneuronal cell lines in an RNA-dependent manner (*10*−*13*). However, the association of FMRP with polyribosomes in brain has been more controversial, one study reporting that FMRP is not in fact associated with polyribosomes in brain extracts (*14*), and it was only recently that this association was proven to exist in brain (*15*, *16*).

FMRP has two autosomal paralogues, the FXR1 and FXR2 proteins (*17*, *18*), with which it shares more than 60% amino acid identity (*19*). The fragile X related gene family formed by FMRP, FXR1, and FXR2 proteins is conserved in mouse, chicken, and *Xenopus*; however, only a single *dfmr1* gene is present in *Drosophila* (ref *19* and references cited therein). Like FMRP, the FXR1 and FXR2 proteins contain two KH domains, but only FXR1 contains an RGG box, whereas FXR2 has an arginine−glycine-rich cluster that does not include any RGG repeat per se. Since they contain similar RNA binding domains, it has been proposed that the FXR1 and FXR2 proteins might compensate for the FMRP function; however, the levels of these proteins are not significantly changed in leukocyte cells of fragile X patients (*20*).

Although the specific mRNA targets of FMRP remain elusive, biochemical studies have identified that FMRP binds with high affinity, using its RGG box domain, to RNA sequences rich in guanine content, which fold into G quartets

† This work was supported by NIH Grant GM074660-01. K.J.Z. and P.E.L. were supported by Duquesne University Research Funds and Undergraduate Summer Research Funds, respectively. G.L.E. was supported by NSERC Grant 298411-2004, Canada, to M.R.M.

* To whom correspondence should be addressed. E-mail: mihailescum@duq.edu. Telephone: (412) 396 1430. Fax: (412) 396 5683.

‡ These authors contributed equally to this work.

§ Duquesne University.

|| Acadia University.

10.1021/bi060209a CCC: $33.50
Published on Web 06/14/2006

(*21*−*23*). G quartet structures consist of guanine tetrads held together by reverse Hoogsteen base pairs, with several G quartet planar structures being able to stack. The formation of such complexes is dependent on the presence of monovalent cations that may lie within the plane of each quartet or between planes. K^+ or Na^+ cations stabilize these structures, whereas their formation is disrupted by the presence of Li^+ (*24*). It has also been shown more recently using in vitro RNA selection that FMRP uses its KH2 domain to bind to a synthetic RNA that harbors a loop−loop kissing complex. The RNA kissing complex is bound by the FMRP KH2 domain with lower affinity than the affinity between its RGG box and G quartet RNA; notably, however, only the kissing complex RNA is able to disrupt the FMRP−polyribosome association and not the G quartet RNA (*25*). Despite the fact that G quartet RNA recognition is not necessary for the FMRP polyribosomal association, the findings that the majority of RNAs that coimmunoprecipitate with FMRP and have altered polyribosome association profiles in the absence of FMRP contain G quartets (*21*, *22*) argue for the relevance of these structural elements in the fragile X syndrome. Thus, in this study we have performed a detailed thermodynamic analysis of the interactions between the FMRP RGG box domain and G quartet forming RNA. Sc1 RNA, which was used in this study as a model system for FMRP−G quartet RNA recognition, had been previously shown to be bound with high affinity by both the full-length FMRP and by its RGG box domain (*21*). We have determined that the FMRP RGG box binding increases the stability of the G quartet RNA structure significantly. Interestingly, we found that the G quartet recognition is necessary but not sufficient for the FMRP RGG box binding to this RNA target, indicating that additional interactions of the peptide, possibly with the stem and/or stem−G quartet junction region, are required. This study also investigated if the G quartet recognition is a more general property of the RGG box domain by analyzing the binding of the RGG box peptides of other RNA binding proteins to G quartet forming RNA.

MATERIALS AND METHODS

Sample Preparation. The unlabeled RNA oligonucleotides (Sc1 and Munc13 site 1) were synthesized by in vitro T7 RNA polymerase transcription reactions using synthetic DNA templates (Trilink Biotechnologies, Inc.), as described (*26*). The RNAs were purified by PAGE and electroelution and were extensively dialyzed against 10 mM Tris (pH 7.5) or 10 mM cacodylic acid (pH 6.5), containing either 150 mM KCl or 150 mM LiCl.

The 2-aminopurine-labeled RNAs were purchased from Dharmacon, Inc., and were resuspended in sterile deionized water. Sc1-15AP RNA was constructed by replacing the adenine at position 15 in Sc1 by 2-aminopurine (2AP) (highlighted in red in Figure 1). Sc1-sh is a shorter version of Sc1-15AP, in which the stem region (shaded in Figure 1B) is missing. Prior to use, all RNA samples were annealed by heating at 95 °C for 5 min, followed by bench cooling.

The FMRP, FXR1, FXR2, and ICP27 RGG box peptides were chemically synthesized and purified by the Peptide Synthesis Unit at the University of Pittsburgh Bioengineering Center.

UV Spectroscopy Thermal Denaturation. The UV spectroscopy experiments were performed on a Varian Cary 3E spectrophotometer equipped with a Peltier cell. The RNA UV thermal denaturation profiles were determined by varying the temperature in the range 20−95 °C at a rate of 0.2 °C/min and measuring the absorbance at 295 nm every degree. Following annealing, the RNA samples were transferred into 200 μL microcuvettes to which a layer of mineral oil (Sigma) was added to prevent evaporation. To determine if the conformation of Sc1 RNA is intramolecular or intermolecular, the melting temperature of its G quartet structure was recorded at different RNA concentrations in the range 3−20 μM, in either 10 mM Tris (pH 7.5) or 10 mM cacodylic acid (pH 6.5) containing 150 mM KCl.

The complexes formed by Sc1 and the RGG box domains of FMRP, FXR1, FXR2, or ICP27 proteins were prepared by mixing 6 μM Sc1 RNA with RGG box peptide in a 1:1 ratio, followed by a 30 min equilibration period. The melting profiles of these complexes were determined by the protocol described above for free Sc1 RNA.

The thermodynamic parameters of Sc1 and Sc1-15AP G quartet structures were determined by fitting the G quartet dissociation transition present in their UV melting curves to eq 1, which assumes a two-state model:

$$A(T) = \frac{A_U + A_F e^{-\Delta H^\circ/RT} e^{\Delta S^\circ/R}}{e^{-\Delta H^\circ/RT} e^{\Delta S^\circ/R} + 1} \quad (1)$$

where A_U and A_F represent the absorbance of the unfolded and native G quartet RNA, respectively.

Fluorescence Spectroscopy. All fluorescence spectroscopy experiments were performed on a J. Y. Horiba Fluoromax-3 equipped with variable temperature control. The excitation wavelength was set at 310 nm, and the fluorescence emission spectra were recorded from 330 to 450 nm, with an averaging time of 0.1 s.

The fluorescence thermal denaturation profile of Sc1-15AP was determined by monitoring the 2AP steady-state fluorescence changes upon temperature increase from 20 to 95 °C. The melting temperature was obtained by fitting the fluorescence melting curve to eq 1, in which A_U and A_F were replaced by F_U and F_F, which represent the steady-state fluorescence of the 2AP reporter in the unfolded and native G quartet RNA, respectively.

The binding of the RGG box peptides of FMRP, FXR1, FXR2, and ICP27 to Sc1-15AP was determined by monitoring the changes in the steady-state fluorescence of 2AP upon titrations of increasing amounts of the RGG peptide to a fixed concentration of the RNA (typically 150 nM). The binding dissociation constant, K_d, was determined by fitting the binding curves to the equation:

$$F = 1 + (I_B/I_F - 1)[(K_d + [P]_t + [RNA]_t) - \sqrt{(K_d + [P]_t + [RNA]_t)^2 - 4[RNA]_t[P]_t}]/2[RNA]_t \quad (2)$$

where I_F and I_B represent the steady-state fluorescence intensities of the free and bound Sc1-15AP, $[RNA]_t$ is the total concentration of Sc1-15AP, and $[P]_t$ is the total RGG box peptide concentration.

The binding of the RGG box peptides to Sc1-15AP in the presence of a 10-fold excess of unlabeled Munc13 site 1 RNA was measured in a similar manner.

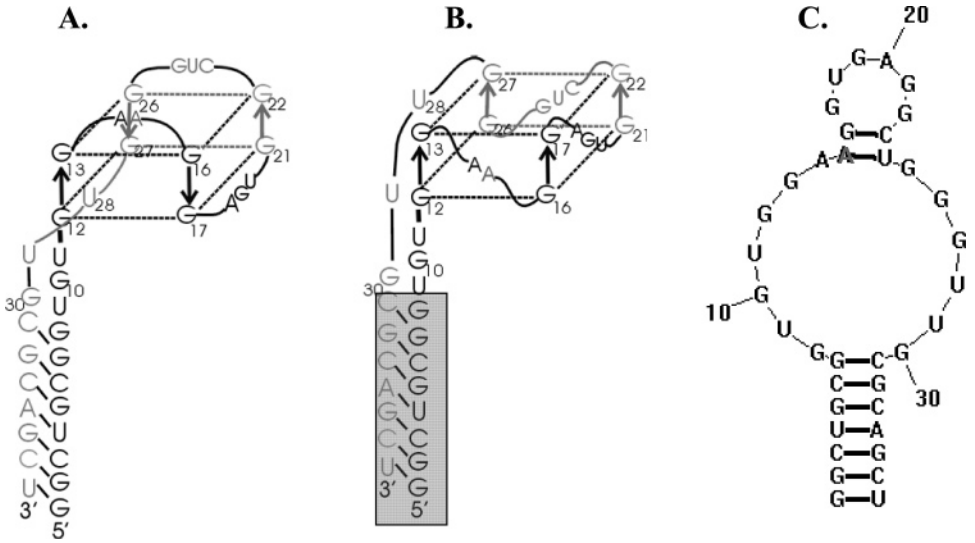

FIGURE 1: (A) Schematic representation of the antiparallel structure of Sc1 RNA (adapted from ref *21*). (B) Proposed parallel G quartet structure; the shaded region is absent from the sequence of Sc1-sh. (C) Secondary structure prediction of Sc1 RNA in the absence of K^+, generated using Zuker's algorithm (*36*). Adenine at position 15, shown in red in all structures, is replaced by 2-aminopurine in Sc1-15AP and Sc1-sh.

To determine the thermodynamic parameters for FMRP RGG box binding to Sc1-15AP, $K_{obs} = 1/K_d$ was determined at different temperatures in the range 25−40 °C by fitting the binding curves to eq 2. The standard enthalpy and entropy of binding were determined from the slope and intercept of the graph:

$$R \ln K_{obs} = \Delta S^\circ_b - (1/T)\Delta H^\circ_b \quad (3)$$

Circular Dichroism Spectroscopy. The circular dichroism (CD) spectroscopy measurements were performed on a Jasco J-710 spectropolarimeter. Following annealing, 10 μM Sc1 RNA in 10 mM cacodylic acid, pH 6.5, and 150 mM KCl in an 800 μL volume was transferred to a 1 cm path length cuvette and equilibrated in the spectropolarimeter at 25 °C. The scans were performed in the range 210−350 nm, with each trace representing an average of a series of six scans with a 1 s response time and a 2 nm bandwidth. The blank spectrum recorded for the buffer was subtracted from the collected data. The same parameters were used to record the CD spectrum of the FMRP RGG box−Sc1 complex, which was prepared by mixing 10 μM Sc1 RNA in a 1:1 ratio with the FMRP RGG box, followed by a 30 min equilibration time. The CD data for the FMRP RGG box−Sc1 complex was corrected by subtraction of the CD spectrum recorded for the free FMRP RGG box.

NMR Spectroscopy. The one-dimensional ^{1}H NMR spectrum of Sc1-sh RNA was recorded on a 500 MHz Varian Unity Plus spectrometer at 29 °C, using the jump-and-return pulse sequence for water suppression (27). The Sc1-sh concentration was 65 μM in 10 mM cacodylic acid at pH 6.5, and 150 mM KCl at a 90% H_2O/10% D_2O ratio. The maximum of excitation was set at 11 ppm, and the recycling delay was 2 s.

Electrophoretic Mobility Gel Shift (EMSA). Sc1 and Sc1-15AP RNAs were mixed in a 1:1 (or 1:2) ratio with the RGG box peptides of the FMRP, FXR1, FXR2, or ICP27 proteins, and following their equilibration for 25 min, the complexes were run on a 15% acrylamide native gel at 60 V for an average time of 3 h. Both the gel and running buffer contained 75 mM KCl. The gels were visualized by UV shadowing at 254 nm using an AlphaImager HP (AlphaInnotech, Inc.).

RESULTS

Sc1 RNA Forms an Intramolecular G Quartet Structure. Sc1 RNA has been proposed to contain a G quartet fold as well as a stem region (Figure 1A) (*21*), and the presence of these secondary structure elements was confirmed by ^{1}H NMR spectroscopy (*28*) and UV spectroscopy (*29*). However, two Sc1 conformers, a monomer and a dimer, are reported to coexist in an equimolar ratio in solution (*28*). It is well documented in the literature that G quartet forming sequences can fold in vitro into alternate secondary structures, with experimental conditions such as pH of the buffer, concentration and type of ions, oligonucleotide concentration, temperature, annealing procedure, etc. playing a role in determining the fraction of one conformer versus the other. We began this study by optimizing each of these parameters (data not shown), and we were able to identify the experimental conditions that promote the folding of Sc1 RNA mainly as a single conformer, with a minimum contribution from the second conformation, as illustrated by its migration pattern on a native gel (Figure 2, lane 4).

We next determined the UV spectroscopy thermal denaturation profile of Sc1 RNA in the presence of KCl and LiCl, respectively, by monitoring the absorbance changes upon increasing the temperature. These experiments were recorded at 295 nm, a wavelength sensitive to G quadruplex dissociation (30). The UV spectroscopy melting curves of 6 μM Sc1 RNA folded in the presence of 150 mM KCl or 150 mM LiCl are quite different (Figure 3A). The 36−60 °C hypochromic transition observed in the presence of K^+ ions was assigned to the melting of the G quartet structure (*31*). This transition is absent from the Sc1 UV melting curve measured in the presence of Li^+ ions that disrupt the formation of G quadruplexes. Our fluorescence melting experiments of Sc1-15AP RNA, which report only on the melting of the G quartet structure, confirm this assignment (see next section).

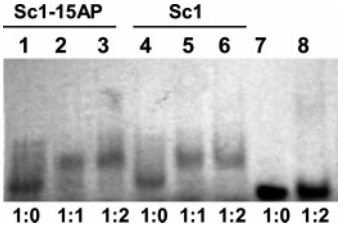

FIGURE 2: Electrophoretic mobility shift analysis of the FMRP RGG box interactions with Sc1 and Sc1-15AP RNA. The RNA concentration was 20 μM for both Sc1-15AP (lane 1) and Sc1 (lane 4). The FMRP RGG box added in 1:1 and 1:2 ratios shifted Sc1-15AP (lanes 2 and 3) and Sc1 (lanes 5 and 6) in a similar manner. Munc13 site 1 RNA was used as a negative control (lanes 7 and 8). Both the gel and running buffer contained 75 mM KCl. The gel was visualized by UV shadowing at 254 nm.

The 60−85 °C hyperchromic transition was assigned to the melting of the Sc1 stem, based on the disappearance of this transition from the UV melting profile of a truncated Sc1 RNA that lacks the stem (ref *31* and this paper).

To confirm that the main conformation we observed for Sc1 RNA is monomeric, we have measured the melting temperature, T_m, of its G quartet structure at different RNA concentrations in the range 3−17 μM. For *intermolecular* species (with n number of strands), $1/T_m$ depends linearly on the natural logarithm of the total RNA concentration (c_T):

$$\frac{1}{T_m} = \frac{R(n-1)}{\Delta H^\circ_{vH}} \ln c_T + \frac{\Delta S^\circ_{vH} - (n-1)R \ln 2 + R \ln n}{\Delta H^\circ_{vH}} \quad (4)$$

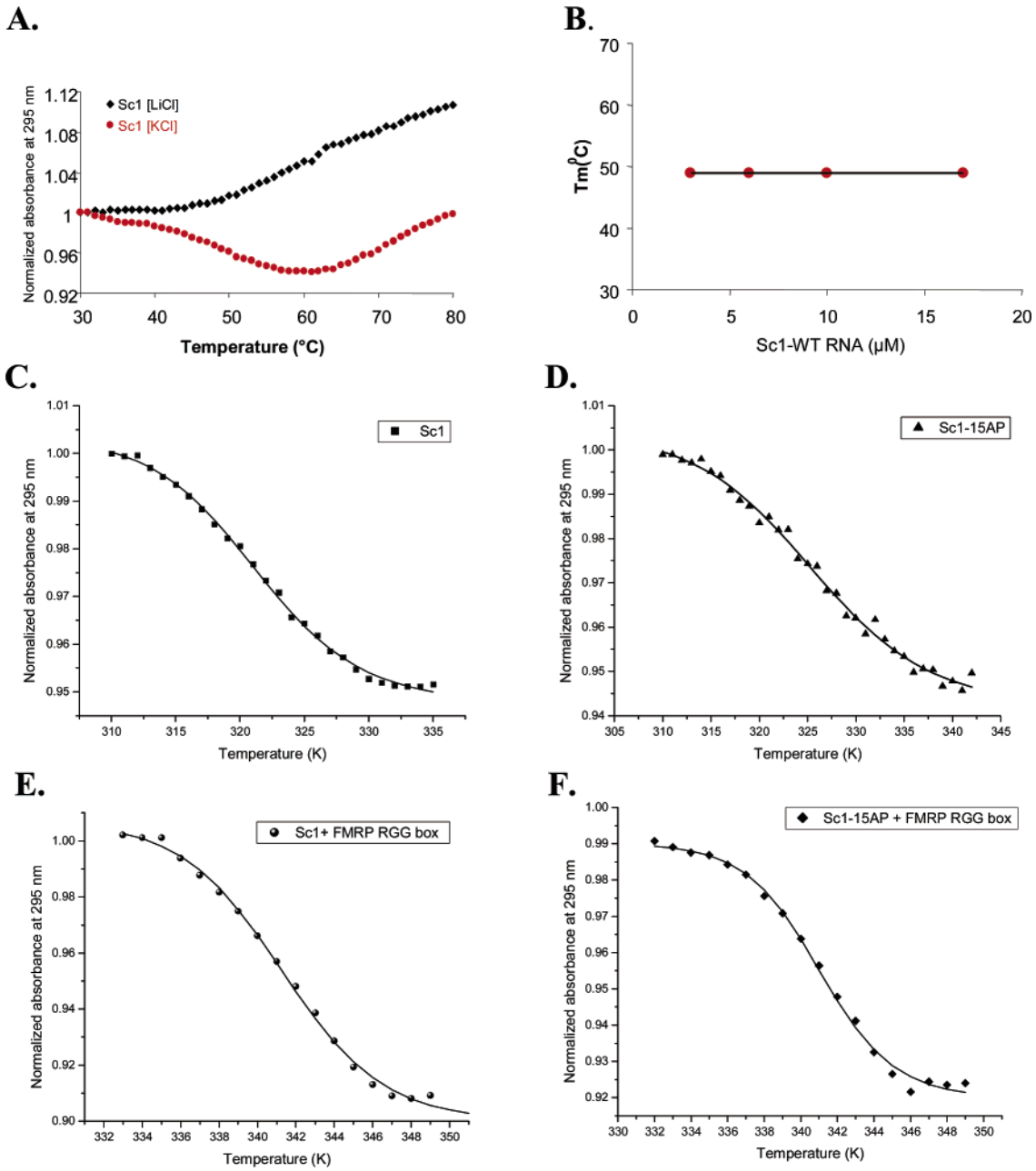

FIGURE 3: (A) UV melting curves of Sc1 RNA in 10 mM Tris, pH 7.5, containing either 150 mM KCl (red circles) or 150 mM LiCl (black diamonds). (B) The melting temperature of the G quartet structure in Sc1 is independent of the RNA concentration. (C−F) The G quartet dissociation hypochromic transitions in the UV melting curves of Sc1 RNA (C), Sc1-15AP (D), the Sc1−FMRP RGG complex (E), and the Sc1-15A−FMRP RGG complex (F). The solid lines in panels C−F represent best fits using eq 1, and the thermodynamic parameters for G quartet formation are summarized in Table 1.

Table 1: Thermodynamic Parameters for G Quartet Structure Formation

molecule	T_m (°C)	$\Delta H°_f$ (kcal/mol)	$\Delta S°_f$ (cal mol^{-1} K^{-1})	$\Delta G°_f$ (kcal/mol)
Sc1	48.2 ± 0.6	−49.8 ± 2.3	−155.0 ± 7.3	−3.6 ± 0.2
Sc1-15AP	52.4 ± 2.1	−35.7 ± 2.9	−109.8 ± 8.8	−3.0 ± 0.3
Sc1-sh	48.9 ± 0.1	−50.8 ± 0.3	−157.8 ± 0.9	−3.8 ± 0.1
Sc1 + FMRP RGG	68.3 ± 1.1	−87.6 ± 5.9	−256.5 ± 17.4	−11.1 ± 0.8
Sc1-15AP + FMRP RGG	68.0 ± 1.5	−113.3 ± 8.4	−332.3 ± 24.5	−14.3 ± 1.1

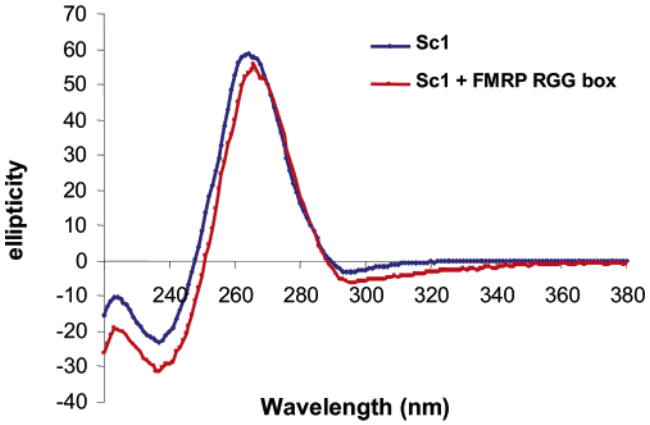

FIGURE 4: CD spectra of free Sc1 RNA (blue trace) and the FMRP RGG box−Sc1 complex (red trace), respectively. The RNA concentration was 10 μM, in 10 mM cacodylic acid at pH 6.5 plus 150 mM KCl, and the spectra were acquired at 25 °C.

where R is the gas constant and $\Delta H°_{vH}$ and $\Delta S°_{vH}$ are the van't Hoff thermodynamic parameters. For *intramolecular* species, T_m is independent of the total RNA concentration c_T: $n = 1$ and $1/T_m = \Delta S°_{vH}/\Delta H°_{vH}$ (*32*).

As illustrated in Figure 3B, the G quartet melting temperature remains constant (~49 °C) at all RNA concentrations investigated, indicating that Sc1 RNA forms *intramolecular* G quartets.

The standard enthalpy, entropy, and free energy of Sc1 G quartet formation were obtained by fitting the 36−60 °C hypochromic transition present in its UV melting profile in 150 mM KCl to eq 1, which assumes a two-state model (Figure 3C and Table 1). The value of the enthalpy of G quartet formation, $\Delta H° = -49.8 \pm 2.3$ kcal/mol, is consistent with the presence of two G quartet planes in the structure of Sc1 RNA (Figure 1A), since for most oligonucleotides, the enthalpy of formation of a single G quartet plane (measured in experimental conditions similar to those used in this study) ranges from −18 to −25 kcal/mol (compiled in ref *32*). The standard Gibbs free energy of G quartet formation at 298 K ($\Delta G° = -3.6 \pm 0.2$ kcal/mol) is also consistent with such a structure (*32*).

We have used CD spectroscopy to obtain additional information about the fold of the G quartet structure of Sc1 RNA. The CD spectrum of Sc1 in 10 mM cacodylic acid, pH 6.5, and 150 mM KCl shows a positive peak at 264 nm and a negative peak at 234 nm, both signatures of parallel G quartet folds (Figure 4). Antiparallel G quartet folds exhibit a positive signal around 295 nm and a negative signal around 260 nm, features absent from the CD spectrum of Sc1 RNA. Thus, our CD data suggest that Sc1 forms a parallel-type G quadruplex structure. However, the existence of such a parallel structure can be confirmed only by high-resolution structural studies, as there are examples in the literature in which the CD data suggested parallel-type structures for intramolecular G quadruplexes that were antiparallel (*33*, *34*).

Fluorescence Spectroscopy Studies of Sc1-15AP RNA. Next, we employed fluorescence spectroscopy to measure the thermodynamic parameters of FMRP RGG box binding to Sc1 RNA. In these studies we used Sc1-15AP RNA, which was constructed by replacing the adenine at position 15 in Sc1 with the highly fluorescent purine analogue 2AP (position highlighted in red in Figure 1). The steady-state fluorescence of 2AP is very sensitive to its environment, in particular to stacking interactions, with the fluorescent properties of the 2AP singlet excited state in the context of a DNA molecule being strongly dependent on the electron transfer quenching process from G (*35*). The 2AP inserted at position 15 is predicted to be part of the G quartet surrounding loops in Sc1-15AP, folded in the presence of K^+, and involved in a Watson−Crick base pair with U24, in the presence of Li^+, which does not promote G quartet formation (Figure 1). Thus, we anticipated that the steady-state fluorescence of this 2AP reporter will increase upon the formation of the G quartet elements, as it is likely that the π stacking of the bases within the G quartet surrounding loops is highly distorted.

To determine if the 2AP insertion perturbs the RNA structure and stability, we have measured the thermodynamic parameters for G quartet formation in Sc1 and Sc1-15AP. The UV spectroscopy melting profiles of Sc1-15AP in the presence of either K^+ or Li^+ ions are very similar to those of Sc1 (data not shown). The standard enthalpy, entropy, and free energy ($\Delta H°$, $\Delta S°$, and $\Delta G°$) for G quartet formation in Sc1-15AP were determined by fitting the UV hypochromic transition corresponding to G quartet dissociation to eq 1 (Figure 3D and Table 1). Although Sc1-15AP has a slightly higher melting temperature than Sc1 RNA (52.4 ± 2.1 versus 48.2 ± 0.6 °C), its G quartet structure is less stable than that of Sc1 RNA as indicated by a slightly larger value of the Gibbs free energy for G quartet formation at 298 K (−3.0 ± 0.3 versus −3.6 ± 0.2 kcal/mol). These small differences in the thermodynamic parameters of G quartet formation in Sc1 and Sc1-15AP indicate that the 2AP insertion did not cause major perturbations of the structure and stability of Sc1 RNA.

As expected, a 5-fold increase in the steady-state fluorescence of Sc1-15AP was observed when the RNA was folded in 10 mM Tris, pH 7.5, and 150 mM KCl versus 150 mM LiCl (Figure 5A). We attribute this change in fluorescence to the different environments in which the 2AP reporter exists: a G-quartet surrounding loop in the presence of K^+ and a Watson−Crick base pair in the presence of Li^+. We have ruled out the possibility that this difference is due to an intrinsic salt dependence of the steady-state fluorescence of 2AP since the fluorescence of 2AP solutions in K^+ versus Li^+ buffers remained constant (data not shown). Thus, we have determined that the 2AP in Sc1-15AP reports directly on the formation of the G quartet structure.

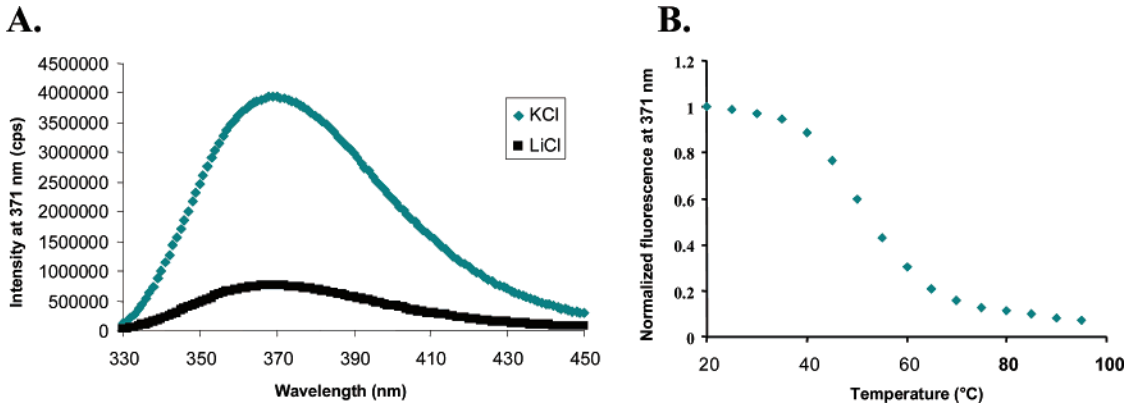

FIGURE 5: (A) Steady-state fluorescence of Sc1-15AP in 10 mM Tris at pH 7.5 plus 150 mM KCl (green trace) or 150 mM LiCl (black trace). The excitation was set at 310 nm, and the emission spectrum was recorded in the range 330−450 nm. (B) Fluorescence thermal denaturation profile of Sc1-15AP in 10 mM cacodylic acid at pH 6.5 plus 150 mM KCl, recorded by monitoring the change in the steady-state fluorescence of 2-AP upon increasing the temperature in the range 20−95 °C.

We have also measured the fluorescence spectroscopy thermal denaturation profile of Sc1-15AP in the presence of 150 mM KCl in the temperature range 20−95 °C. Only a single transition with a T_m of ~52 °C is present in the fluorescence melting curve (Figure 5B), which we attribute to the melting of the G quartet structure in Sc1-15AP. Since 2AP is a microscopic reporter, the transition corresponding to the melting of the Sc1-15AP stem (observed by UV spectroscopy) is not present in the fluorescence melting curve.

FMRP RGG Box Binding to Sc1 and Sc1-15AP RNA. The binding of the FMRP RGG box to Sc1 and Sc1-15AP was studied by electrophoretic mobility shift assay (EMSA) and, in the case of Sc1-15AP, also by fluorescence spectroscopy.

Figure 2 shows the EMSA pattern of FMRP RGG box binding in 1:1 and 2:1 ratios to Sc1-15AP (lanes 2 and 3) and Sc1 RNA (lanes 5 and 6). As a negative control for binding, we have used the Munc13 site 1 RNA (lanes 7 and 8) (*21*). Since the FMRP RGG box binds in a manner similar to Sc1-15AP and Sc1 RNA, Sc1-15AP was further used in fluorescence spectroscopy experiments to obtain information about the thermodynamics of FMRP RGG box binding.

Figure 6A shows the binding curve of the FMRP RGG box to Sc1-15AP, determined at 25 °C by titrating increasing amounts of the RGG peptide to a fixed concentration of Sc1-15AP. The steady-state fluorescence of the 2AP fluorophore in Sc1-15AP decreases upon the titration of the FMRP RGG peptide, indicating that this reporter is sensitive to the binding event. A dissociation constant, K_d, of 7.9 ± 4.0 nM was determined by fitting the binding curve to eq 2.

To determine the thermodynamic parameters of FMRP RGG box binding to Sc1-15AP, we measured the binding association constant $K_{obs} = 1/K_d$ as a function of temperature in the range 25−40 °C. The standard enthalpy and entropy of binding (summarized in Table 2) were extracted from the slope and intercept of the plot of ln K_{obs} versus of $1/T$ (Figure 6B and eq 3).

We next tried to quantify the electrostatic nature of binding in the FMRP RGG box−Sc1-15AP complex by measuring K_{obs} at different salt concentrations. We expected that electrostatics would play an important role in the binding of the FMRP RGG box to Sc1-15AP, considering the negatively charged phosphate backbone of the RNA and the positively charged arginine residues of the RGG peptide. This electrostatic component should be reflected in the dependence of the association constant, K_{obs}, on the monovalent salt concentration, M^+, known as the salt dependence: $\partial \log K_{obs}/\partial \log [M^+]$. However, as illustrated in Figure 6C, the binding of the FMRP RGG box to Sc1-15AP was not affected by increasing the salt concentration in the range 150−1000 mM KCl, indicating that electrostatic interactions do not play a dominant role in the binding of the FMRP RGG box to Sc1-15AP RNA. Similar results were obtained using EMSA to analyze the binding between the FMRP RGG box and Sc1 RNA at various KCl concentrations in the range 150−600 mM (data not shown).

G Quartets Are Required but Not Sufficient for FMRP RGG Box Binding. Also shown in Figure 6A is the titration of increasing amounts of the FMRP RGG box into a solution of Sc1-sh RNA, which is a shorter version of Sc1-15AP that lacks the stem region. Sc1-sh was originally designed as a negative control for the fluorescence spectroscopy measurements of binding, since it has been reported that, in the absence of the stem, the FMRP RGG box does not bind to Sc1 (*21*). Our fluorescence and EMSA (data not shown) results confirm that the stem is required for FMRP RGG binding to Sc1-15AP; however, we were surprised to find that this shorter Sc1-sh RNA still folds into a G quadruplex structure. The UV thermal denaturation profile of Sc1-sh in 10 mM Tris at pH 7.5 and 150 mM KCl has a single hypochromic transition that corresponds to G quartet dissociation (Figure 7A). The thermodynamic parameters of G quartet formation in Sc1-sh were obtained by fitting this transition to eq 1 and are summarized in Table 1.

The presence of a G quartet structure in Sc1-sh was also confirmed in the one-dimensional ^{1}H NMR spectrum of Sc1-sh, which contains imino proton resonances in the region 10−12 ppm, signatures of G quartets (Figure 6B).

The FMRP RGG Box Binding Increases the Stability of the G Quartet Structure in Sc1 and Sc1-15AP RNA. To determine if the FMRP RGG box alters the conformation of Sc1 RNA, we have compared its CD spectrum with that of the FMRP RGG box−Sc1 complex. As illustrated in Figure 4, the two CD spectra are very similar, indicating that there are no major structural changes in Sc1 RNA upon binding of the FMRP RGG box.

We then investigated if the binding of the FMRP RGG box has any effect upon the stability of Sc1 RNA. Stabiliza-

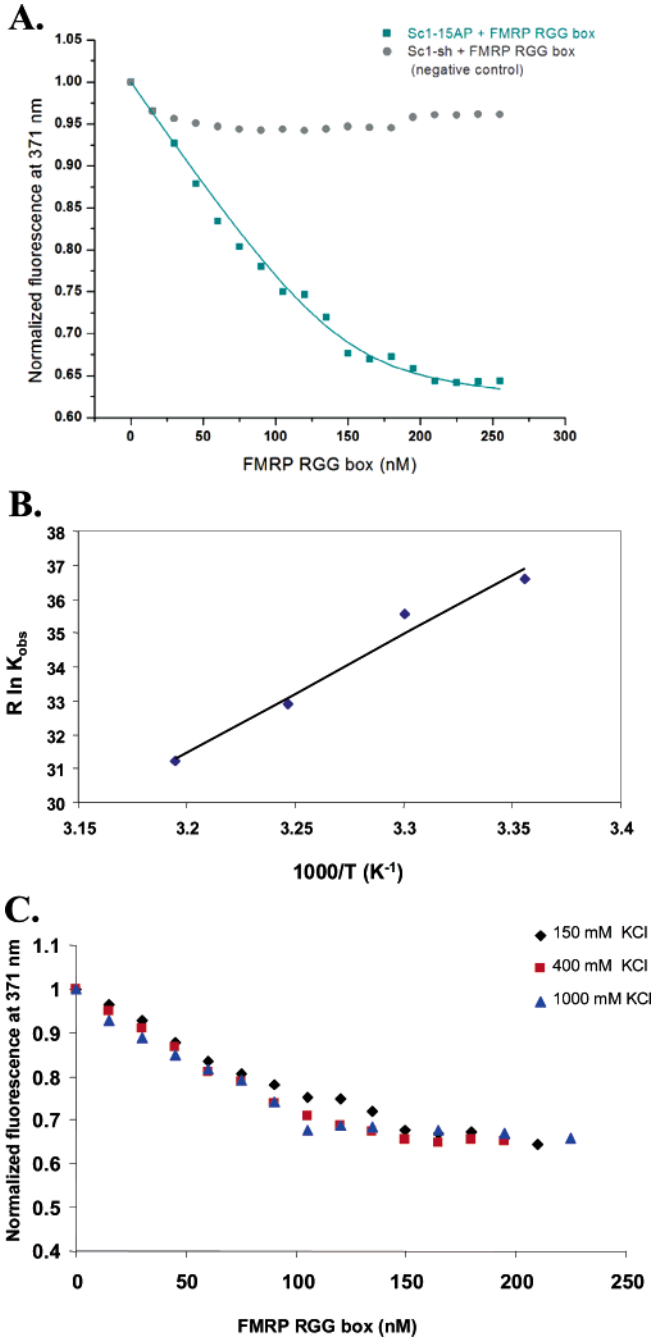

FIGURE 6: (A) Binding curve of the FMRP RGG box to Sc1-15AP determined by fluorescence spectroscopy (green squares). Increasing increments of the FMRP RGG box were titrated in a solution of 150 nM Sc1-15AP in 10 mM cacodylic acid at pH 6.5 plus 150 mM KCl. The solid line represents the best fit using eq 2, from which a $K_d = 7.9 \pm 4.0$ nM was determined. Also shown is the titration curve for Sc1-sh (gray circles) which was used as a negative control. (B) van't Hoff plots of steady-state fluorescence measurements for the Sc1-15AP−FMRP RGG box complex in 10 mM cacodylic acid at pH 6.5 plus 150 mM KCl; the binding thermodynamic parameters are summarized in Table 2. (C) Binding curves of the FMRP RGG box to Sc1-15AP measured at different salt concentrations: 150 mM KCl (black diamonds), 400 mM KCl (red squares), and 1000 mM KCl (blue triangles).

tion or destabilization of nucleic acids by proteins can be readily monitored as an increase or decrease of the nucleic acid melting temperature T_m. Thus, we compared the G quartet melting temperature of free Sc1 or Sc1-15AP with that of the Sc1−FMRP RGG box complex (and Sc1-15AP−FMRP RGG box, respectively). The 36−60 °C UV hypochromic transition corresponding to G quartet dissociation in Sc1 (or Sc1-15AP) is shifted to 60−73 °C in the melting curve of the Sc1−FMRP RGG box complex (or Sc1-15AP−FMRP RGG box complex) (Figure 3E,F). The T_m value of the G quartet structure of Sc1 increases from ~49 °C in the free RNA to ~68 °C when the RNA is bound by the FMRP RGG box, indicating that peptide has a stabilizing effect on the G quartets. These G quartet dissociation transitions were fitted to eq 1, and as summarized in Table 1, the stabilization effect of the FMRP RGG peptide is reflected by a change of the free energy from -3.6 ± 0.2 kcal/mol for the free Sc1 RNA to -11.2 ± 0.2 kcal/mol for the RNA−peptide complex. A similar change in free energy is observed for Sc1-15AP (Table 1).

Table 2: Thermodynamic Parameters for FMRP RGG Box Binding to Sc1-15AP RNA

$\Delta H°_b$ (kcal/mol)	$\Delta S°_b$ (cal mol^{-1} K^{-1})	$\Delta G°_b$ (kcal/mol)
-35.0 ± 4.0	-80.6 ± 13.3	-10.0 ± 0.8

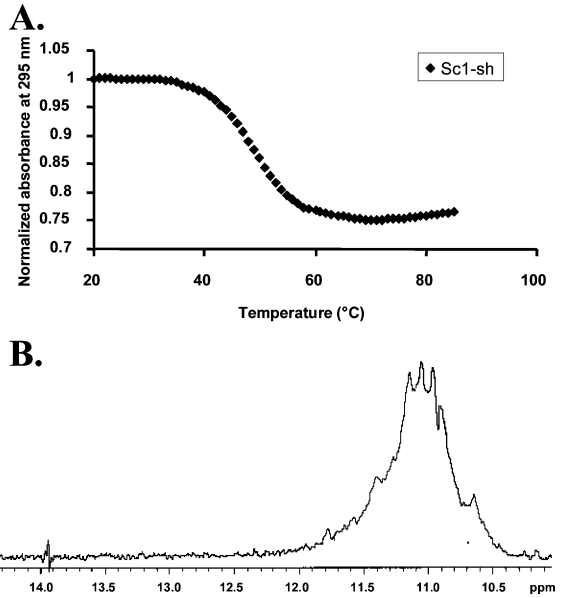

FIGURE 7: (A) UV thermal denaturation profile of 6 μM Sc1-sh RNA in 10 mM Tris at pH 7.5 plus 150 mM KCl. (B) Imino proton resonance region of the 1D ^{1}H NMR spectrum of Sc1-sh RNA in 10 mM cacodylic acid at pH 6.5 plus 150 mM KCl.

How Specific Is the Recognition of Sc1 RNA by the FMRP RGG Box? One of the goals of this study was to investigate if G quartet recognition is a more general feature of the RGG box RNA binding motif, by studying the interactions of different RGG box peptides derived from other proteins with G quartet forming RNA sequences. By investigating the binding of these RGG boxes to the FMRP RNA target Sc1, we also sought to determine if the recognition of the G quartet forming Sc1 RNA is unique to the FMRP RGG box. Thus, we have selected for this study the RGG boxes of FXR1 and of the herpes simplex virus 1 protein ICP27 and the arginine−glycine cluster of the FXR2 protein, whose sequences are shown in Table 3. Although the FXR2 protein does not have an actual RGG box, but only an RG cluster, it was still included in this study since the protein is an autosomal paralogue of FMRP. The essential nuclear protein ICP27 was selected since it has been reported that it binds with high affinity in vivo to RNA sequences containing

Table 3: Primary Sequences of the RGG Box Peptides Used in This Study

FMRP RGG box	RRGDGRR**RGG**GGRGQGGRG**RGG**GFKGNDDHSR
FXR1 RGG box	HQRDSRRRPGGRGRSVSGGRG**RGG**P**RGG**KSS
FXR2 RG cluster	TRGEESRRRPTGGRGRGPPPAPRP
ICP27 RGG box	QPA**RGG**RRGRRRGRG**RGG**PGAAP

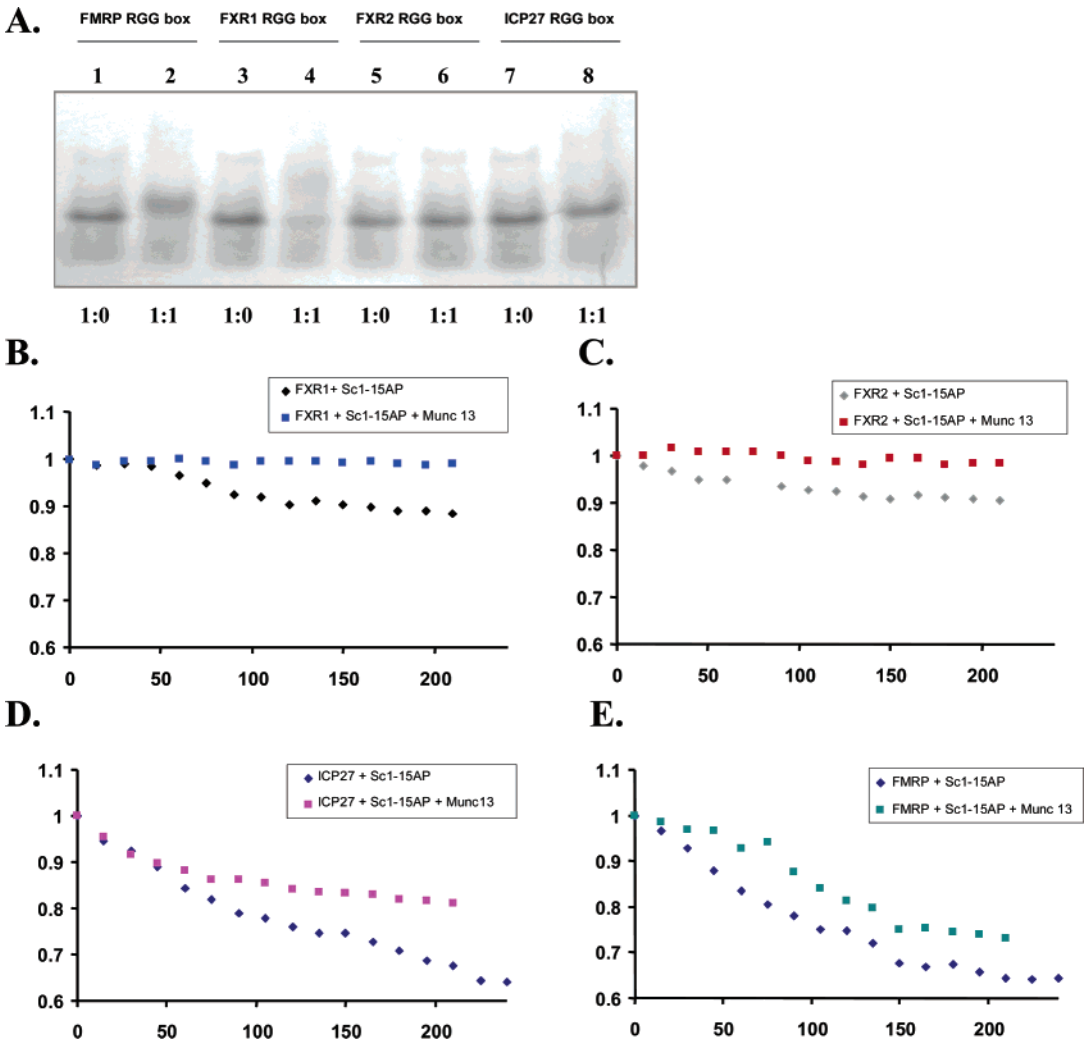

FIGURE 8: (A) Electrophoretic mobility shift analysis of the FMRP RGG box (lanes 1 and 2), FXR1 RGG box (lanes 3 and 4), FXR2 RG cluster (lanes 5 and 6), and ICP27 RGG box (lanes 7 and 8) binding to Sc1 RNA. The RNA concentration was 40 μM, and the RGG box peptides were added in 1:1 ratios. Both the gel and running buffer contained 75 mM KCl, and the gel was visualized by UV shadowing at 254 nm. Binding of the RGG boxes of FXR1 (B), FXR2 (C), ICP27 (D), and FMRP (E) to Sc1-15AP in the absence (diamonds) and presence of a 10-fold excess of Munc13 site 1 RNA (squares).

multiple G repeats that have the potential to fold into G quartets (*37*). The mechanisms by which ICP27 regulates genes are not known; however, there is evidence that it is an RNA binding protein and that the protein domain responsible for this activity is an RGG box-like short arginine−glycine-rich sequence (*38*).

We initially used EMSA to test if the RGG boxes of FXR1 and ICP27 and the RG cluster of FXR2 bind to Sc1 RNA. As illustrated in Figure 8A, in the presence of the FXR1 RGG box the band corresponding to free Sc1 RNA is diminished (lanes 3 and 4), indicating that this peptide binds Sc1 RNA. However, no defined band is present for the FXR1 RGG box−Sc1 complex, indicating that Sc1 is bound with lower affinity by the FXR1 RGG box than the FMRP RGG box (compare lanes 2 and 4). The FXR2 RG cluster does not bind Sc1 RNA (lanes 5 and 6), whereas the ICP27 RGG box binds with high affinity to Sc1 RNA as indicated by the shift of the free Sc1 RNA band (lanes 7 and 8). Note that the binding of the ICP27 RGG box results in a smaller shift of the free Sc1 RNA band since the ICP27 RGG peptide has 23 amino acids as compared with the FMRP RGG box, which has 32 amino acids.

We next investigated the binding of these peptides to Sc1-15AP via fluorescence spectroscopy. To determine if the binding to Sc1-15AP is specific, the binding curves were also determined in the presence of a 10-fold excess of unlabeled Munc13 site 1 RNA. As illustrated in Figure 8B, the binding of the FXR1 RGG box to Sc1-15AP is largely nonspecific, since in the presence of an excess of Munc13 RNA the binding is completely abolished. Similarly, the FXR2 RG cluster shows minimal binding to Sc1-15AP, and this is completely abolished in the presence of unlabeled Munc13 RNA (Figure 8C). However, the ICP27 RGG box shows stronger binding to Sc1-15AP (Figure 8D), and the

fit of the binding curve measured in the absence of Munc13 RNA to eq 2 resulted in a $K_d = 54.5 \pm 17.4$ nM. The RGG boxes of both ICP27 and FMRP show considerable binding, even in the presence of a 10-fold excess of Munc13 RNA, indicating that they bind Sc1-15AP specifically (Figure 8D,E). It is interesting to note that although ICP27 binds specifically to Sc1-15AP, it does not affect the stability of the G quartets, as the melting temperature of this structure remains invariant upon binding of the ICP27 RGG box (data not shown).

DISCUSSION

In this report we have performed a thermodynamic analysis of the interactions between the FMRP RGG box and G quartet forming Sc1 RNA. We have identified the experimental conditions in which Sc1 RNA folds mainly as a single species and used thermodynamic methods to determine that this species is monomeric. Our thermodynamic data (Table 1) support the presence of two G quartet planes in the structure of Sc1 RNA, as originally proposed (*21*). However, our CD spectroscopy results (Figure 4) suggest that the G quartets are of parallel type, and we propose for Sc1 RNA the structure illustrated in Figure 1B. This structure is of a similar type with the intramolecular G quadruplex parallel-stranded structure determined for the promoter region of the c-MYC oncogene (*39*). The c-MYC promoter structure has three parallel G tetrads flanked by three stable side loops that are well defined in the NMR spectra, with the 3′-flanking sequence forming a stable foldback conformation that caps the top end of the G quadruplex structure. The Sc1 RNA structure is likely to be more complicated since the 3′-flanking sequence has to reach back to form a stem with the 5′-end of the molecule.

Thermodynamics of FMRP RGG Box Binding to Sc1 RNA. We have employed fluorescence spectroscopy to thermodynamically analyze the binding of the FMRP RGG box to Sc1-15AP RNA, which has been constructed by inserting the 2AP highly fluorescent adenine analogue at position 15 in the sequence of Sc1. The UV thermal denaturation profiles of Sc1 and Sc1-15AP show the same transitions, with the thermodynamic parameters for G quartet formation in the two molecules having similar values. These results indicate that the 2AP insertion did not cause significant perturbations of the structure and stability of Sc1 RNA. The adenine at position 15 is predicted to be part of a G quartet surrounding loop when Sc1-15AP is folded in the presence of KCl and involved in a Watson−Crick base pair when Sc1-15AP is folded in the presence of LiCl (Figure 1B,C). We have determined that the steady-state fluorescence of 2AP increases 5-fold when Sc1-15AP is folded in the presence of 150 mM KCl, as compared with 150 mM LiCl, indicating that this site reports on the G quartet structure formation (Figure 5A). Moreover, the steady-state fluorescence of 2AP is also sensitive to the thermal denaturation of the molecule, showing a transition with a melting temperature of ~52 °C, in very good agreement with the G quartet melting temperature determined by UV spectroscopy (Figure 5B).

We have used fluorescence spectroscopy to measure the binding of the FMRP RGG box to Sc1-15AP, determining a K_d of 7.9 ± 4.0 nM for the FMRP RGG box−Sc1-15AP complex at 25 °C (Figure 6A), which is similar to the 10 nM value determined by Darnell et al. (*21*) for the binding of full-length FMRP to Sc1 RNA. Thus, the association between the FMRP RGG box and Sc1-15AP RNA is characterized by a standard Gibbs free energy of $\Delta G^\circ = -11.0 \pm 0.8$ kcal/mol. The free energy of binding provides only an overall description of the system, whereas for a more complete understanding of the forces that drive the FMRP RGG box−Sc1-15AP association, the definition of the enthalpic and entropic contributions to the free energy of binding is required. These thermodynamic parameters of binding were determined by measuring the association constant of the FMRP RGG box−Sc1-15AP complex, $K_{obs} = 1/K_d$, as a function of temperature (Figure 6B and Table 2). The association between the FMRP RGG box and Sc1-15AP RNA is enthalpically driven ($\Delta H^\circ = -35.0 \pm 4.0$ kcal/mol) with an unfavorable entropic contribution ($T\Delta S^\circ = -24.0 \pm 3.4$ kcal/mol). Favorable enthalpy changes originate typically from hydrogen bonds and hydrophobic and electrostatic interactions, whereas unfavorable entropy changes are associated with a decrease in conformational flexibility. We have determined that the formation of the FMRP RGG box−Sc1-15AP complex is insensitive to high salt concentrations (Figure 6C), indicating that electrostatic contributions do not play a major role in the binding of Sc1-15AP. Thus, it is more likely that the favorable enthalpy contribution to the standard Gibbs free energy of binding originates from hydrogen bonds and hydrophobic interactions. These findings are unusual, since the importance of electrostatic interactions in RNA binding by proteins is well documented in the literature (*40*−*44*), but not unprecedented. The *Trypanosoma brucei* mitochondrial Y-box protein RBP16, which contains a cold-shock domain at its N-terminus and an RGG box-like domain at its C-terminus, binds to its guide RNA gA6 target in a relatively insensitive manner with respect to high salt concentrations (*45*). It is interesting to note that, in the case of RBP16, the treatment of the protein with phenylglyoxal (PGO) that specifically modifies arginine residues by interacting with α-amino groups completely abolished gA6 RNA binding, indicating that one or more arginine residues are involved in the RBP16−gA6 interaction. However, in the case of this protein, it has not been shown unambiguously that only the RGG box-like domain is responsible for gA6 binding. In contrast, the FMRP RGG box binds Sc1 RNA with the same affinity as the full-length protein (*21*), indicating that the recognition of the G quartet forming Sc1 RNA resides entirely in its RGG box. Thus, the findings that electrostatic interactions do not play a dominant role in the binding between the positive RGG box peptide and the negatively charged Sc1 RNA suggest that hydrogen bonds between the arginine residues of the FMRP RGG box and specific bases in Sc1-15AP make a major contribution to the favorable enthalpy of binding. The importance of these hydrogen bonds in the FMRP RGG box binding to Sc1 RNA is supported by the recent findings that, upon the posttranslational methylation of some of its arginine residues, the binding of the FMRP RGG box to Sc1 RNA is greatly reduced but not completely abolished (*46*). Thus, additional interactions contribute to the formation of the FMRP RGG box and Sc1 RNA complex, with one possible candidate being the phenylalanine at position 24 in the FMRP RGG peptide (position 550 in the human FMRP) that might be involved

in stacking interactions with bases in Sc1 RNA. It is worthwhile to mention that although RGG motifs are quite different in various proteins, in many cases the RGG repeat is immediately followed by a phenylalanine (RGGF or RGGGF) or tyrosine residue (RGGY or RGGGGY) (summarized in ref *47*). Thus, the conserved aromatic residues in the RGG box might be important for intercalation in the RNA structure, with the hydrogen bonds between the arginine residues and specific RNA bases being involved in the proper positioning of these aromatic residues.

We have determined that the binding of the FMRP RGG box increases the stability of the G quartet structure significantly, as reflected by an increase in the melting temperature of these structures from 49 °C in the free Sc1 RNA (or Sc1-15AP) to 68 °C in the FMRP RGG box−Sc1 complex (Figure 3C−F). It has been reported previously that the binding of the nucleolin RGG box to the double-stranded DNA $A_{25}T_{25}$ stabilized its structure, resulting in an increase of its melting temperature from ~40 to 50 °C (*47*), with this increase in the duplex stability being attributed to the better screening of the DNA backbone phosphates by the positively charged RGG peptide. To our knowledge this is the first report showing that an RGG box RNA binding domain contributes to an increase in the stability of an RNA G quadruplex structure. Moreover, our results suggest that the increase in the stability of the G quartet structure induced by the RGG box peptide binding is not due to nonspecific electrostatic interactions but to specific interactions between the peptide and RNA.

G Quartet Recognition in RNA Is Not Sufficient for FMRP RGG Box Binding. The FMRP RGG box does not bind to Sc1-sh, a shorter version of Sc1-15AP from which the stem region is missing, in good agreement with reports in the literature indicating that the stem region is required for binding (*21*). However, we were surprised to find that, in the presence of 150 mM KCl, Sc1-sh folds into a G quadruplex structure, as indicated by its UV thermal denaturation profile at 295 nm (Figure 7A) and by the presence of imino proton resonances in the 11−12 ppm region of its 1D ^{1}H NMR spectrum (Figure 7B). It is likely that this G quadruplex structure in Sc1-sh is similar to that existing in the full-length Sc1, as they have the same thermodynamic parameters of G quartet formation (Table 1). Thus, it seems that only G quartet recognition is not sufficient for FMRP RGG box binding, suggesting that additional interactions of the peptide with the stem region and/or junction region between the G quartet and stem have to be present.

The Recognition of the G Quartet Forming Sc1 RNA Is Not Unique to the FMRP RGG Box. We have investigated the binding of two other RGG boxes, derived from the FXR1 protein and the herpes simplex virus 1 ICP27 protein, as well as of the FXR2 RG cluster to Sc1 RNA and Sc1-15AP. We intended to determine, first, if G quartet recognition is a general property of the RGG box RNA binding motif and, second, how unique is the recognition between Sc1 RNA and the FMRP RGG box. Our EMSA and fluorescence results (Figure 9) indicate that the FXR1 RGG box and the FXR2 RG cluster bind nonspecifically to Sc1 RNA. These results support the idea that the electrostatic interactions are not dominant in the binding between the FMRP RGG box and Sc1 RNA, as the number of positive charges (originating from arginine residues) in the FMRP and FXR1 RGG boxes and FXR2 RG cluster is similar (nine in FXR1 and FMRP RGG boxes and seven in the FXR2 RG cluster). Interesting, however, were the results that the viral protein ICP27 binds specifically Sc1-15AP, albeit with a larger K_d than the FMRP RGG box (54.5 ± 17.4 versus 7.9 ± 4.0 nM). The analysis of the sequences of these two RGG boxes shows that they contain two RGG repeats spaced by nine amino acids (mainly arginines and glycines), a property not shared by the FXR1 RGG box. Thus, it is tempting to speculate that this precise spacing between the RGG repeats might be relevant for the proper positioning of the arginine and or aromatic residues involved in specific Sc1 RNA recognition. While this result indicates that the recognition of Sc1 RNA is not unique to the FMRP RGG box, it is worth mentioning that the increase in the stability of the Sc1 G quartet structures occurs only upon the binding of the FMRP RGG box and not the ICP27 RGG box.

Our results also indicate that G quartet RNA recognition is not a general feature of the RGG box motif, involving some protein and/or RNA sequence specificity.

CONCLUSIONS

This study reports on a detailed thermodynamic analysis of the interactions between the FMRP RGG box and Sc1 RNA, which was used as a model system to gain information about the recognition between the RGG box RNA binding motif and G quartet forming RNA. Our results point toward hydrogen bonding and hydrophobic interactions playing a major role in the favorable enthalpy contribution to the binding free energy, with minor contributions from electrostatic interactions. Interestingly, we have determined that the FMRP RGG box binding increases the stability of the Sc1 RNA G quartet structure. Our preliminary results of the FMRP interactions with two other potential in vivo RNA targets (L. Menon and S. Mader) hint to the possibility that the protein might use its RGG box domain to selectively affect the stability of the G quartet structures present in these RNA molecules. The G quartet RNA recognition has been proposed to be relevant in the FMRP binding to its RNA targets (*21*−*23*, *48*). However, our findings that the G quartet Sc1 RNA recognition is not unique to the FMRP RGG box suggest that additional interactions of the other RNA binding domains of the protein will allow for a complete discrimination of these RNA targets. One such interaction could possibly involve the KH2 domain−RNA kissing complex recognition (*25*).

ACKNOWLEDGMENT

We thank Denyse Clace for involvement in the early stages of this project, Michelle Trim for preparation of the Munc13 site 1 RNA, and Lakshmi Menon for help in acquiring the CD spectroscopy data. We also thank Dr. Bruce Armitage for allowing us to use the CD spectropolarimeter at Carnegie Mellon University and Dr. John Marino (CARB/NIST) for critical comments on the manuscript.

REFERENCES

1. Crawford, D. C., Acuna, J. M., and Sherman S. (2001) FMR1 and the fragile X syndrome: human genome epidemiology review, *Genet. Med. 3*, 359−371.
2. Jin, P., and Warren, S. T. (2003) New insights into fragile X syndrome: from molecules to neurobehaviors, *Trends Biochem. Sci. 28*, 152−158.

3. Devys, D., Lutz, Y., Rouyer, N., Bellocq, J. P., and Mandel, J. L. (1993) The FMR-1 protein is cytoplasmic, most abundant in neurons and appears normal in carriers of a fragile X permutation, *Nat. Genet. 4*, 335−340.
4. Bagni, C., and Greeenough, W. T. (2005) From mRNP trafficking to spine dysmorphogenesis: the roots of fragile X syndrome, *Nat. Rev. Neurosci. 6*, 376−387.
5. Ashley, C. T., Wilkinson, K. D., Reines, D., and Warren, S. T. (1993) FMR1 protein: conserved RNP family domains and selective RNA binding, *Science 262*, 563−566.
6. Siomi, H., Siomi, M., Nussbaum, R., and Dreyfuss, G. (1993) The protein product of the fragile X gene, FMR1, has characteristics of an RNA-binding protein, *Cell 74*, 291−198.
7. Adinolfi, S., Ramos, A., Martin, S. R., Dal Piaz, F., Pucci, P., Bardoni, B., Mandel, J. L., and Pastore, A. (2003) The N-terminus of the fragile X mental retardation protein contains a novel domain involved in dimerization and RNA binding, *Biochemistry 42*, 10437−10444.
8. Ramos, A., Hollingworth, D., Adinolfi, S., Castets, M., Kelly, G., Frenkiel, T. A., Bardoni, B., and Pastore, A. (2006) The structure of the N-terminal domain of the fragile x mental retardation protein: a platform for protein−protein interaction, *Structure 14*, 21−31.
9. Eberhart, D. E., and Warren, S. T. (1996) Molecular basis of fragile X syndrome, in *Cold Spring Harbor Symposia on Quantitative Biology*, Vol. LXI, pp 679−687, Cold Spring Harbor Laboratory Press, Cold Spring Harbor, NY.
10. Eberhart, D. E., Malter, H. E., Feng, Y., and Warren, S. T. (1996) The fragile X mental retardation protein is a ribonucleoprotein containing both a nuclear localization and nuclear export signals, *Hum. Mol. Genet. 5*, 1083−1091.
11. Khandjian, E. W., Corbin, F., Woerly, S., and Rousseau, F. (1996) The fragile X mental retardation protein is associated with ribosomes, *Nat. Genet. 12*, 91−93.
12. Tamanini, F., Meijer, N., Verheij, C., Willems, P. J., Galjaard, H., Oostra, B. A., and Hoogeveen, A. T. (1996) FMRP is associated to the ribosomes via RNA, *Hum. Mol. Genet. 5*, 809−813.
13. Feng, Y., Absher, D., Eberhart, D. E., Brown, V., Malter, H. E., and Warren, S. T. (1997) FMRP associates with polyribosomes as an mRNP, and the I304N mutation of severe fragile X syndrome abolishes this association, *Mol. Cell 1*, 109−118.
14. Zalfa, F., Giorgi, M., Primerano, B., Moro, A., Di Penta, A., Reis, S., Oostra, B., and Bagni, C. (2003) The fragile X syndrome protein FMRP associates with BC1 RNA and regulates the translation of specific mRNAs at synapses, *Cell 112*, 317−327.
15. Stefani, G., Fraser, C. E., Darnell, J. C., and Darnell, R. B. (2004) Fragile X mental retardation protein is associated with translating polyribosomes in neuronal cells, *J. Neurosci. 24*, 7272−7276.
16. Khandjian, E. W., Huot, M.-E., Tremblay, S., Davidovic, L., Marzoui, R., and Bardoni B. (2004) Biochemical evidence for the association of fragile X mental retardation protein with brain polyribosomal ribonucleoparticles, *Proc. Natl. Acad. Sci. U.S.A. 101*, 13357−13362.
17. Siomi, M. C., Siomi, H., Sauer, W. H., Srinivasan, S., Nussbaum, R. L., and Dreyfuss, G. (1995) FXR1, an autosomal homolog of the fragile X mental retardation gene, *EMBO J. 14*, 2401−2408.
18. Zhang, Y., O'Connor, J. P., Siomi, M. C., Srinivasan, S., Dutra, A., Nussbaum, R. L., and Dreyfuss, G. (1995) The fragile X mental retardation syndrome protein interacts with novel homologs FXR1 and FXR2, *EMBO J. 14*, 5358−5366.
19. Kirkpatrick, L. L., McIlwain, K. A., and Nelson, D. L. (2001) Comparative genomic sequence analysis of the FXR gene family: FMR1, FXR1 and FXR2, *Genomics 78*, 169−177.
20. Kaufmann, W. E., Cohen, S., Sun, H. T., and Ho, G. (2001) Molecular phenotype of fragile X syndrome: FMRP, FXRPs, and protein targets, *Micros. Res. Tech. 57*, 135−144.
21. Darnell, J. C., Jensen, K. B., Jin, P., Brown., V., Warren, S. T., and Darnell, R. B. (2001) Fragile X mental retardation protein targets G quartet mRNAs important for neuronal function, *Cell 107*, 489−499.
22. Brown, V., Jin, P., Ceman, S., Darnell J. C., O'Donnel, W. T., Tenenbaum, S. A., Jin, X., Feng, Y., Wilkinson, K. D., Keene, J. D., Darnell, R. B., and Warren, S. T. (2001) Microarray identification of FMRP-associated brain mRNAs and altered mRNA translational profiles in fragile X syndrome, *Cell 107*, 477−487.
23. Schaeffer, C., Bardoni, B., Mandel, J.-L., Ehresmann, B., Ehresmann, C., and Moine, H. (2001) The fragile X mental retardation protein binds specifically to its mRNA via a purine quartet motif, *EMBO J. 20*, 4803−4813.
24. Williamson, J. R., Raghuraman, M. K., and Cech, T. R. (1989) Monovalent cation-induced structure of telomeric DNA: the G-quartet model, *Cell 59*, 871−880.
25. Darnell, J. C., Fraser, C. E., Mostovetsky, O., Stefani, G., Jones, T. A., Eddy, S. R., and Darnell, R. B. (2005) Kissing complex RNAs mediate interaction between the fragile-X mental retardation protein KH2 domain and brain polyribosomes, *Genes Dev. 19*, 903−918.
26. Milligan, J. F., and Uhlenbeck, O. C. (1989) Synthesis of small RNAs using T7 RNA polymerase, *Methods Enzymol. 180*, 51−62.
27. Plateau, P., and Gueron, M. (1982) Exchangeable protons without base line distortion using a new strong pulse sequence, *J. Am. Chem. Soc. 104*, 7310−7311.
28. Ramos, A., Hollingworth, D., and Pastore, A. (2003) G-quartet-dependent recognition between the FMRP RGG box and RNA, *RNA 9*, 1198−1207.
29. Marin, V., and Armitage, B. A. (2005) RNA guanine quadruplex invasion by complementary and homologous PNA probes, *J. Am. Chem. Soc. 127*, 8032−8033.
30. Mergny, J.-L., Phan, A.-T., and Lacroix, L. (1998) Following G-quartet formation by UV spectroscopy, *FEBS Lett. 435*, 74−78.
31. Marin, V. L., and Armitage, B. A. (2006) *Biochemistry 45*, 1745−1754.
32. Hardin, C. G., Perry, A. G., and White, K. (2001) Thermodynamic and kinetic characterization of the dissociation and assembly of quadruplex nucleic acids, *Biopolymers 56*, 147−194.
33. Jing, N., Marchand, C., Liu, J., Mitra, R., Hogan, M., and Pommier, Y. (2000) Mechanism of inhibition of HIV-1 integrase by G-tetrad-forming oligonucleotides *in vitro*, *J. Biol. Chem. 275*, 21460−21467.
34. Dapic, V., Abdomerovic, V., Marrington, R., Peberdy, J., Rodger, A., Trent, J. O., and Bates, P. J. (2003) Biophysical and biological properties of quadruplex oligodeoxyribonucleotides, *Nucleic Acids Res. 31*, 2097−2107.
35. Kelley, S. O., and Barton, J. K. (1999) Electron transfer between bases in double helical DNA, *Science 283*, 375−381.
36. Zuker, M. (2003) Mfold web server for nucleic acid folding and hybridization prediction, *Nucleic Acids Res. 31*, 3406−3415.
37. Sokolowski, M., Scott, J. E., Heaney, R. P., Patel, A. H., and Clements, J. B. (2003) Identification of herpes simplex virus RNAs that interact specifically with regulatory protein ICP27 in vivo, *J. Biol. Chem. 278*, 33540−33549.
38. Mears, W. E., and Rice, S. A. (1996) The RGG box motif of the herpes simplex virus ICP27 protein mediates an RNA-binding activity and determines in vivo methylation, *J. Virol. 70*, 7445−7453.
39. Ambrus, A., Chen, D., Dai, J., Jones, R. A., and Yang, D. (2005) Solution structure of the biologically relevant G-quadruplex element in the human c-MYC promoter. Implications for G-quadruplex stabilization, *Biochemistry 44*, 2048−2058.
40. Bougie, I., Parent, A., and Bisaillon, M. (2004) Thermodynamics of ligand binding by the yeast mRNA-capping enzyme reveals different modes of binding, *Biochem. J. 384*, 411−420.
41. Austin, R. J., Xia, T., Ren, J., Takahashi, T. T., and Roberst, R. W. (2003) Differential modes of recognition in N peptide-BoxB complexes, *Biochemistry 42*, 14957−14967.
42. Köller, J., Muller, U. F., Schmid, B., Missel, A., Kruft, V., Stuart, K., and Göringer, H. U. (1997) An arginine-rich mitochondrial protein that binds to guide RNA with high affinity, *J. Biol. Chem. 272*, 3749−3757.
43. Schindelin, H., Jiang, W., Inouye, M., and Heinemann, U. (1994) Crystal structure of CspA, the major cold shock protein of *Escherichia coli*, *Proc. Natl. Acad. Sci. U.S.A. 91*, 5119−5123.
44. Oubridge, C., Ito, N., Evans, P. R., Teo, C. H., and Nagai, K. (1994) Crystal structure at 1.92 Å resolution of the RNA binding domain of the U1A protein complexed with an RNA hairpin, *Nature 372*, 432−438.
45. Pelletier, M., Miller, M. M., and Read, L. K. (2000) RNA-binding properties of the mitochondrial Y-box protein RBP16, *Nucleic Acids Res. 28*, 1266−1275.
46. Stetler, A., Winograd, C., Sayegh, J., Cheever, A., Patton, E., Zhang, X., Clarke, S., and Ceman. S. (2006) Identification and characterization of the Methyl arginines in the fragile X mental retardation protein Fmrp, *Hum. Mol. Genet. 15*, 87−96.

47. Raman, B., Guarnaccia, C., Nadassy, K., Zakhariev, S., Pintar, A., Zanuttin, F., Frigyes, D., Acatrinei, C., Vindigni, A., Pongor, G., and Pongor, S. (2001) N-omega-arginine dimethylation modulates the interaction between a Gly/Arg-rich peptide from human nucleolin and nucleic acids, *Nucleic Acids Res. 29*, 3377−3384.

48. Darnell, J. C., Warren, S. T., and Darnell, R. B. (2004) The fragile X mental retardation protein, FMRP, recognizes G-quartets, *Ment. Retard. Dev. Disabil. Res. Rev. 10*, 49−52.

BI060209A